Yu.V. Verbovytskyy, I.Yu. Zavaliy, V.V. Berezovets, P.Ya. Lyutyy

# Solid Gas and Electrochemical Hydrogenation Properties of the $R_{1-x}R'_xMgNi_{4-y}Co_y$ (R, R' = Y, La, Ce) Alloys

*Karpenko Physico-Mechanical Institute, NAS of Ukraine, Lviv, Ukraine, yuryvv@bigmir.net*

New $R_{1-x}R'_xMgNi_{4-y}Co_y$ (R, R' = Y, La, Ce; $x = 0.5$; $y = 0, 1, 2$) alloys have been synthesized by powder sintering method, and their crystal structure and hydrogen storage properties have been studied. X-ray diffraction analysis showed that $R_{1-x}R'_xMgNi_{4-y}Co$ alloys belong to the $MgCu_4Sn$-type structure. The synthesized alloys absorb hydrogen at room temperature and hydrogen pressure 0.1 - 10 bar. For some of the studied compounds, the formation of hydrides with cubic and orthorhombic structures was found. Highest hydrogen content is found for the Co-rich compounds: $La_{0.5}Y_{0.5}MgNi_2Co_2H_{5.18}$ and $La_{0.5}Ce_{0.5}MgNi_2Co_2H_{6.48}$. Electrochemical studies showed that Y-based electrode materials exhibit better electrochemical performance comparing with Ce-doped ones. Highest discharge capacity of 292 mA·h/g was observed for $La_{0.5}Y_{0.5}MgNi_3Co$, but the best cyclic stability after 50th cycle of 92 % was seen for $La_{0.5}Y_{0.5}MgNi_2Co_2$. Additionally, obtained results of the electrochemical properties were compared with related compounds. High rate dischargeability of Co-free alloys at I = 1 A/g were twice higher than ones containing cobalt.

**Keywords:** rare earth compounds, magnesium compounds, crystal structure, hydrogen storage, metal hydride electrodes.

## Introduction

Rare earth - magnesium - nickel based hydrogen storage alloys have gained increasing interest as one of the most promising materials for negative electrodes in Ni-MH batteries. Electrochemical discharge capacity of the electrode materials based on the La-Mg-Ni-Co alloy reached 400 mAh/g [1, 2], which is 30 % higher than the capacity of commercial $LaNi_5$-based electrodes. However, the poor cyclic stability (degradation during the cyclic process) is the main problem, which hinders its practical application. Several methods were adopted to improve the cyclic stability of such alloys. Metal substitution, mechanical milling and various preparation techniques are some of them [3-5]. Basically obtained materials are the mixtures of Laves $AB_2$, Haucke $AB_5$ or/and superlattice $(AB_2)_n(AB_5)_m$ phases. Among them the $RMgNi_4$ phases are characterized by good solid gas and electrochemical properties and can be easily prepared by sintering or induction melting methods [6-18]. Recently, the $YMgNi_{4-x}Co_x$ [19], $LaMgNi_{4-x}Co_x$ [20], $NdMgNi_{4-x}Co_x$ [21], $La_{1-x}Nd_xMgNi_{4-y}Co_y$ [22] and $Pr_{1-x}La_xMgNi_{4-y}Co_y$ [23] alloy systems were systematically investigated in our research group. The gas hydrogenation of such alloys shown that the maximum capacity increases linearly with the Co content from ~4 H/f.u. to ~6 H/f.u., however, the Ni/Co substitution has different effect on value of discharge capacity as well as cyclic stability. In the present work a series of hydrogen storage alloys $R_{1-x}R'_xMgNi_{4-y}Co_y$ (R, R' = Y, La, Ce; x = 0.5, y = 0, 1 and 2) were prepared and the effect of metal multiple substitution on gas and electrochemical hydrogenation was studied.

## I. Experimental details

Starting materials for the preparation of the $R_{1-x}R'_xMgNi_{4-y}Co_y$ (R, R' = Y, La, Ce; x = 0.5, y = 0−3) alloys were ingots of La, Ce, Y, Ni, and Co (all with purity ≥99.9 %) and Mg powder (325 mesh, 99.8 %). In the first step, $La_{0.5}R_{0.5}Ni_{4-y}Co_y$ (y = 0−3) alloy precursors were prepared by arc melting in a purified argon

atmosphere. The as-cast $La_{0.5}R_{0.5}Ni_{4-y}Co_y$ buttons were ground in an agate mortar and after obtained powders with size less than 0.04 mm then mixed with Mg powder in certain proportions. Mg was added with 3 wt % excess to compensate for its evaporation loss at high temperatures. The powder mixtures were pressed into pellets with diameter of 10 mm at 10 ton, placed into stainless steel containers and sealed under an Ar atmosphere. Samples further heated up to 800ºC and down to 500 ºC within several days, and annealed at 500 ºC ten days. Structural analysis of the samples was carried out by X-ray powder diffraction (XRD) using a DROM 3M diffractometer (Cu Kα radiation). Crystal structures of the compounds were refined by Rietveld method from the diffraction data using Fullprof software [24]. Elemental composition of the alloys was examined by scanning electron microscopy (SEM) using an EVO 40XVP microscope equipped with Inca Energy 350 spectrometer for energy dispersive X-ray analysis (EDX).

Hydrogen absorption−desorption properties of the alloys were characterized using a Sieverts-type apparatus. The samples were activated by heating up to 200 °C in dynamic vacuum, cooled to room temperature, and then hydrogenated with high-purity hydrogen gas (99.999 %).

The electrode materials made of the alloys were prepared by mixing of with carbonyl Ni powder with the 1:3 wt. ratio. The pellet electrodes with a diameter of 12mm were made by cold-pressing the powder mixture under a pressure of 10 ton/cm² and then sandwiched between two Ni foams with the fixed conductor. Metal hydride electrodes were tested in a three-electrode system. Platinum auxiliary and metal hydride (MH) working electrodes were placed in a glass cell filled with KOH solution (CM=6 M) electrolyte, while the Ag/AgCl reference electrode was connected to the system via an agar bridge. Cycling stability of the MH electrodes was studied galvanostatically at the current densities of 50 mA/g at room temperature. The potential for the charge/discharge was measured between −0.6 V and −1.2 V versus the Ag/AgCl electrode. High rate dischargeability (HRD) was investigated by the discharge of the electrodes at the high current density (up to 1 A/g) until the electrode reaches the potential −0.6 V versus the Ag/AgCl electrode.

## II. Results and discussion

**Sample synthesis and crystal structure of parent alloys**

A series of single phase $R_{1-x}R'_xMgNi_{4-y}Co_y$ intermetallics (IMCs) with $SnMgCu_4$ structure type (space group $F$-$43m$) have been synthesized. In this structure the La and Ce or La and Y atoms occupied the Mg ($4a$) site, the Ni atoms or its statistical mixture with Co are distributed over the Cu ($16e$) site, and the Mg atoms are situated in the Sn ($4c$) positions. The unit-cell
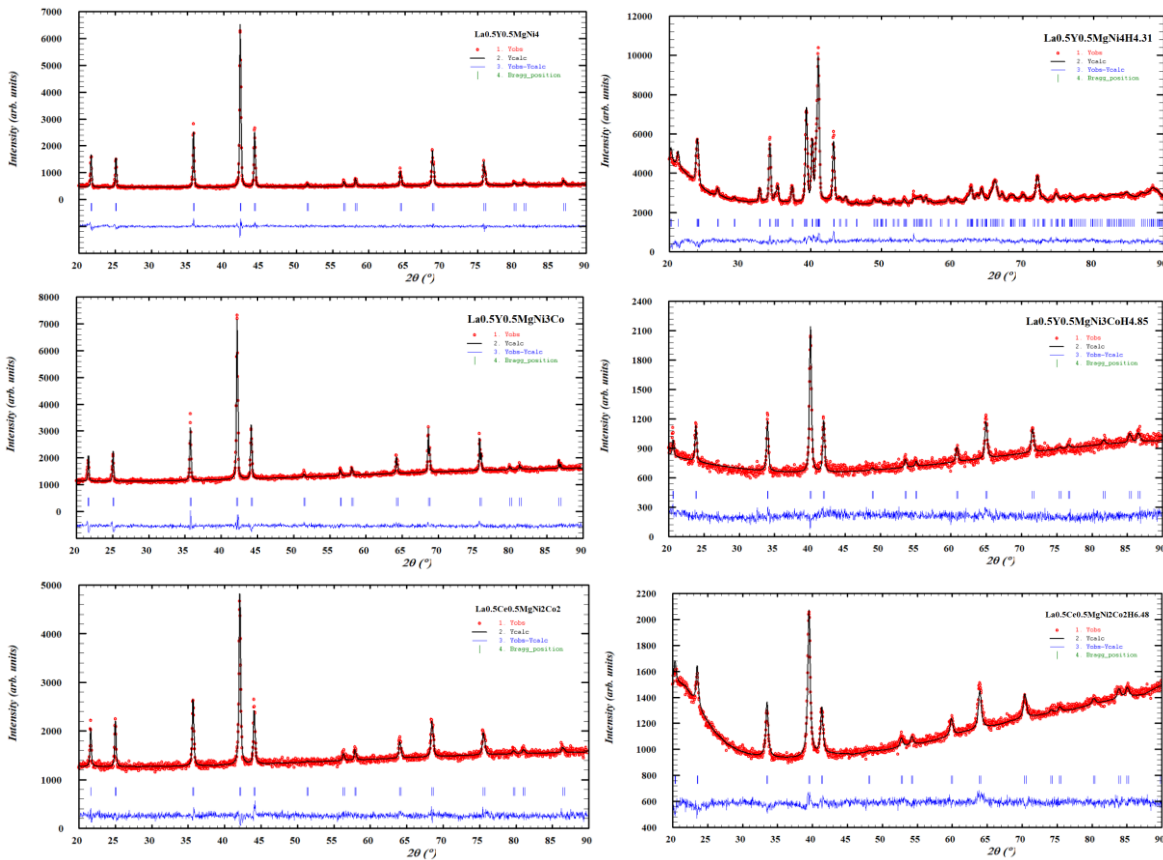


**Fig. 1.** X-ray diffraction patterns of $La_{0.5}Y_{0.5}MgNi_4$, $La_{0.5}Y_{0.5}MgNi_3Co$, $La_{0.5}Ce_{0.5}MgNi_2Co_2$ and their hydrides, $La_{0.5}Y_{0.5}MgNi_4H_{4.31}$, $La_{0.5}Y_{0.5}MgNi_3CoH_{4.85}$, $La_{0.5}Ce_{0.5}MgNi_2Co_2H_{6.48}$.

volume $V$ of $La_{0.5}Y_{0.5}MgNi_{4-y}Co_y$ and $La_{0.5}Ce_{0.5}MgNi_{4-y}Co_y$ IMCs increases almost linearly versus the Co content (Table 1). Alloys with the composition with $y = 3$ and 4 were not prepared and studied in the present paper; however, we did not exclude that above mentioned alloys can be formed as the single phase and belong to certain continues solid solutions. Lattice constants for $La_{0.5}Y_{0.5}MgNi_4$ ($a = 7.0875$ Å) and $La_{0.5}Ce_{0.5}MgNi_4$ ($a = 7.1023$ Å), as an expected, are close to the half sum ($a = 7.090$ Å and $a = 7.095$ Å) of the respective ones for $LaMgNi_4$, $YMgNi_4$ or $CeMgNi_4$ IMCs [25]. XRD patterns of selected alloys are illustrated in Fig. 1.

### Gas solid hydrogenation properties

The $R_{1-x}R'_xMgNi_{4-y}Co_y$ alloys, except for $La_{0.5}Ce_{0.5}MgNi_4$, easily absorb hydrogen at ambient condition (room temperature and maximum pressure 10 bar $H_2$). $La_{0.5}Ce_{0.5}MgNi_4$ slow absorbs hydrogen and it was not formed saturated hydride after 1000 h. Curves of first hydrogenation are presented on Fig. 2. All the investigated alloys have incubation period, but the shortest one can be seen for the $La_{0.5}Ce_{0.5}MgNi_{4-y}Co_y$ alloys. With Co content increasing, for all alloys, improvement of the kinetics of solid-gas hydrogenation was observed. Once they begin absorbing hydrogen, they saturate rapidly and reach their maximum hydrogen capacity. Also, Co-containing compounds absorb more hydrogen then Co-free ones. Last fact can be caused by increasing of unit cell parameters and that is the hydrogen atoms preface to occupy interstices composed by various type of atoms.

### Crystal structure of the hydrides

All the obtained hydrides were exposed to air to passivate the surface and were characterized by XRD. Rietveld refinements of the selected XRD pattern are illustrated in Fig. 1. For Co-free compounds the formation of hydrides with structure transformation was observed (cubic initial compound → orthorhombic hydride). The $La_{0.5}Y_{0.5}MgNi_4H_{4.31}$ hydride was obtained as a single phase hydride with orthorhombic structure. Hydrogenation reaction of the $La_{0.5}Ce_{0.5}MgNi_4$ alloy was not completed, thus two phases were seen in the XRD pattern. The lattice parameters of these phases were successfully calculated and it was suggested that they are hydrides but still with unknown hydrogen content. There were two hydrides, fist hydride is so-called alfa-phase, solid solution of hydrogen in the parent intermetallic, and second one was found with orthorhombic structure (see Table 1). Structure transformation was not observed for
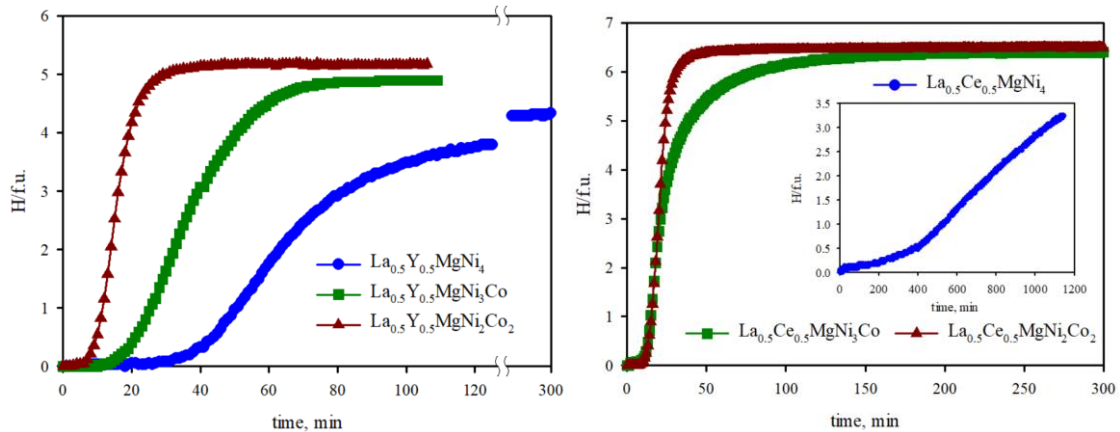


**Fig. 2.** Curves of first hydrogenation of the $R_{1-x}R'_xMgNi_{4-y}Co_y$ alloys.

**Table 1**

Lattice parameters of the parent intermetallics and their hydrides

| No | Phase | $a, b, c$ (Å) | V (Å³) | $\Delta V/V$ (%) | $\Delta V/n_H$ (Å³/n) |
|---|---|---|---|---|---|
| 1. | $La_{0.5}Y_{0.5}MgNi_4$ | 7.0875(3) | 356.03(2) | - | - |
| 2. | $La_{0.5}Y_{0.5}MgNi_3Co$ | 7.1010(3) | 358.06(3) | - | - |
| 3. | $La_{0.5}Y_{0.5}MgNi_2Co_2$ | 7.1090(8) | 359.28(7) | - | - |
| 4. | $La_{0.5}Ce_{0.5}MgNi_4$ | 7.1023(3) | 358.27(2) | - | - |
| 5. | $La_{0.5}Ce_{0.5}MgNi_3Co$ | 7.1112(3) | 359.61(2) | - | - |
| 6. | $La_{0.5}Ce_{0.5}MgNi_2Co_2$ | 7.1172(7) | 360.51(6) | - | - |
| 7. | $La_{0.5}Y_{0.5}MgNi_4H_{4.31}$ | 5.0783(5) 5.4611(7) 7.3789(8) | 204.64(4) | 15.0 | 3.09 |
| 8. | $La_{0.5}Y_{0.5}MgNi_3CoH_{4.85}$ | 7.4553(12) | 414.37(18) | 15.7 | 2.90 |
| 9. | $La_{0.5}Y_{0.5}MgNi_2Co_2H_{5.18}$ | 7.480(3) | 418.6(2) | 16.5 | 2.86 |
| 10. | $La_{0.5}Ce_{0.5}MgNi_4H_x$ | 5.124(4) 5.496(4) 7.492(5) | 211.0(3) | 17.8 | - |
| 11. | $La_{0.5}Ce_{0.5}MgNi_3CoH_{6.40}$ | 7.547(3) | 429.8(3) | 19.5 | 2.74 |
| 12. | $La_{0.5}Ce_{0.5}MgNi_2Co_2H_{6.48}$ | 7.563(2) | 432.5(2) | 20.0 | 2.78 |

**Table 2**

Summarized electrochemical properties for the electrodes

| No | Phase | $C_{max}$, mA·h/g | $C_{50}$, mA·h/g | $S_{50}$, % | $C_{HRD/100}$, mA·h/g | $HRD_{1000}$, % |
|---|---|---|---|---|---|---|
| 1. | $La_{0.5}Y_{0.5}MgNi_4$ | 278 | 230 | 82 | 290 | 42 |
| 2. | $La_{0.5}Y_{0.5}MgNi_3Co$ | 292 | 246 | 84 | 313 | 21 |
| 3. | $La_{0.5}Y_{0.5}MgNi_2Co_2$ | 277 | 256 | 93 | 278 | 18 |
| 4. | $La_{0.5}Ce_{0.5}MgNi_4$ | 217 | 137 | 63 | 219 | 47 |
| 5. | $La_{0.5}Ce_{0.5}MgNi_3Co$ | 241 | 133 | 55 | 265 | 21 |
| 6. | $La_{0.5}Ce_{0.5}MgNi_2Co_2$ | 210 | 126 | 60 | 186 | 11 |
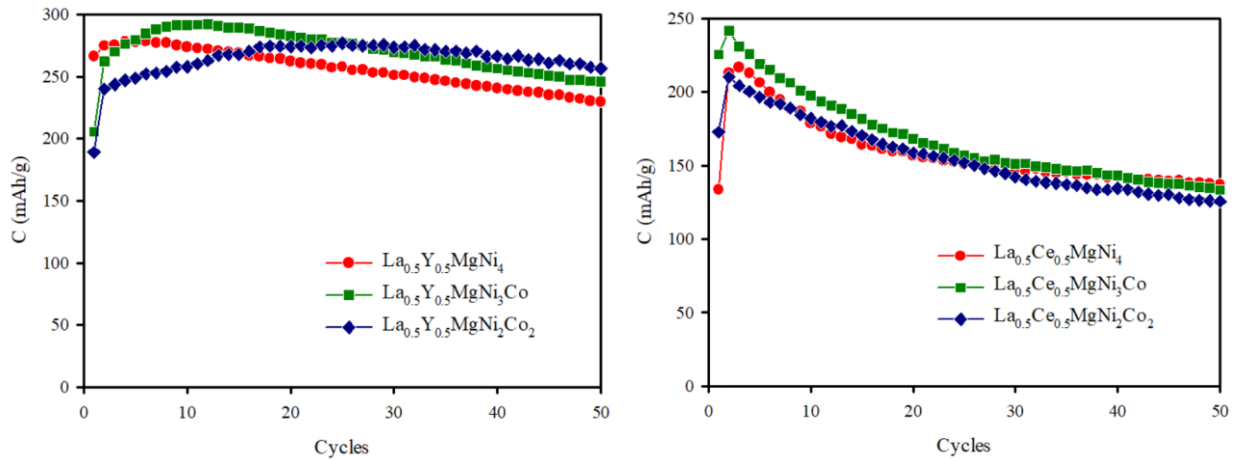


**Fig. 3.** Cyclic stability of the electrodes (discharge current density at I = 50 mA/g).

Co-containing alloys, thus they retain the initial cubic symmetry of the parent compounds. Hydride formation is accompanied by isotropic enlargement of cell parameters of the initial structure. Volume expansion of unit cell for hydrides with initial structure is in the range 15 – 20 % larger than parent structure. In general, volume evolution has good agreement with absorbed amounts of hydrogen. Refined crystallographic parameters of the orthorhombic and cubic hydrides are presented in Table 1.

**Electrochemical properties**

Fig. 3 shows the relationship between the electrochemical discharge capacities and the cycle number measured for $R_{1-x}R'_xMgNi_{4-y}Co_y$ alloys at a charging/discharging current density of 50 mA/g. It is seen that all the electrodes exhibit the superior activation capability, reaching the maximum discharge capacity after a few charging-discharging cycles with exception of $La_{0.5}Y_{0.5}MgNi_2Co_2$ with unknown nature. The highest obtained discharge capacity of 282 mA·h/g is observed for the $La_{0.5}Y_{0.5}MgNi_{4-y}Co_y$ series of the alloys. Discharge capacity of the $La_{0.5}Ce_{0.5}MgNi_{4-y}Co_y$ alloys were not exceeded 250 mA·h/g. Last ones is also characterized by poor capacity retaining rate after 50th cycle. Cyclic stability $S_{50}$ for the $La_{0.5}Ce_{0.5}MgNi_{4-y}Co_y$ electrodes are always less than 65 %, for comparison more 80 % capacities after 50th cycle are retained for the $La_{0.5}Y_{0.5}MgNi_{4-y}Co_y$ electrodes. This can be explained by low corrosion resistance of the Ce-containing alloys comparing with Y-based ones. In general degradation of electrode is attributed to the three factors: first, an oxidation of electrode materials and the formation of

$Mg(OH)_2$ and $La(OH)_3$ surface layers, which decrease the surface electrocatalytic activity and prevent the diffusion of hydrogen into the electrode; second, the formation of stable hydride phases cannot be excluded, this will decrease the discharge capacities of the studied electrode material; third, the pulverization of the electrodes due to the expansion and contraction of the cell volume in the hydrogenation/dehydrogenation cycles, the appeared during this process micro-cracks induces pulverization.

The discharge curves of the $R_{1-x}R'_xMgNi_{4-y}Co_y$ alloy electrodes at 50 mA/g are shown in Fig. 4. It can be seen that each curve, for example at fifth cycle, has a wide discharge potential plateau (based on the oxidation of desorbed hydrogen from the hydride), which shifts toward a more positive potential when nickel atoms substitute by cobalt ones in the alloys. The mid-discharge potential of Co-free alloy electrodes very between -1.0037 and -1.0305 V, while Co containing ones change from -0.9713 to -0.9998 V.

An important parameter of the electrode alloy is its electrochemical kinetics, which is here evaluated by its high rate dischargeability (HRD). The HRD value is calculated according to following formula: HRD = 100 %·$C_{dis}/C_{100}$, where $C_{dis}$ and $C_{100}$ are the discharge capacities of the alloy electrode charged-discharged at the current densities of $I_{dis}$ and 100 mA/g, respectively. Fig. 5 provides the variations of the high rate dischargeability (HRD) of the alloys with the discharge current density, from which it is found that HRD of the $R_{1-x}R'_xMgNi_{4-y}Co_y$ alloy decrease from 42/47 % to 18/11 % when the y value grows from 0 to 2. It indicates
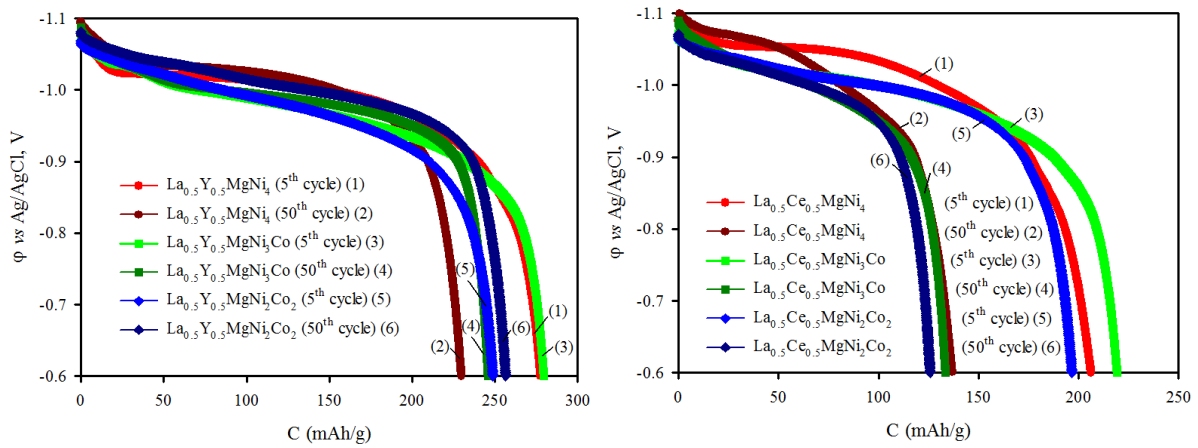
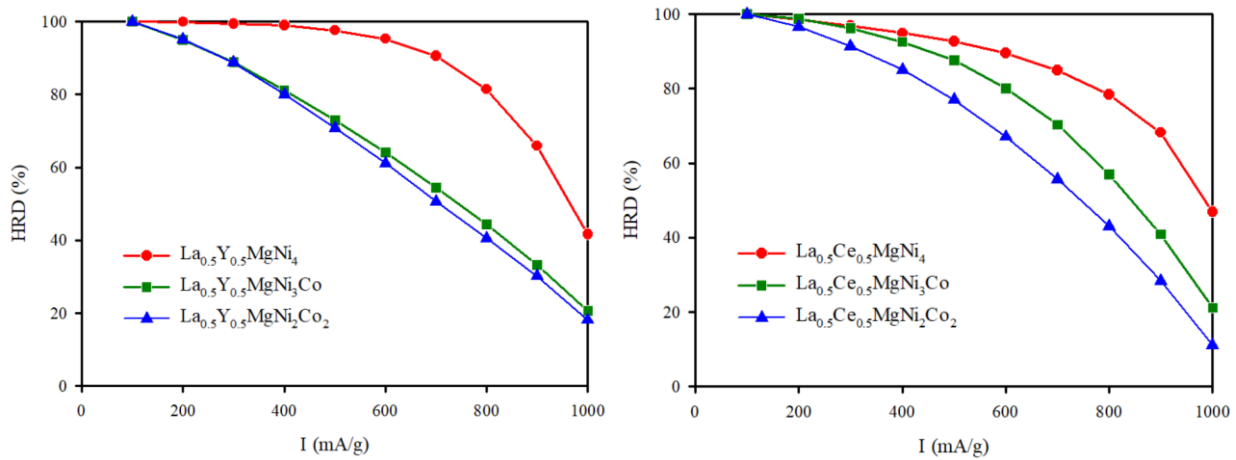**Fig. 4.** The discharge potential curves at discharge density of 50 mA/g.



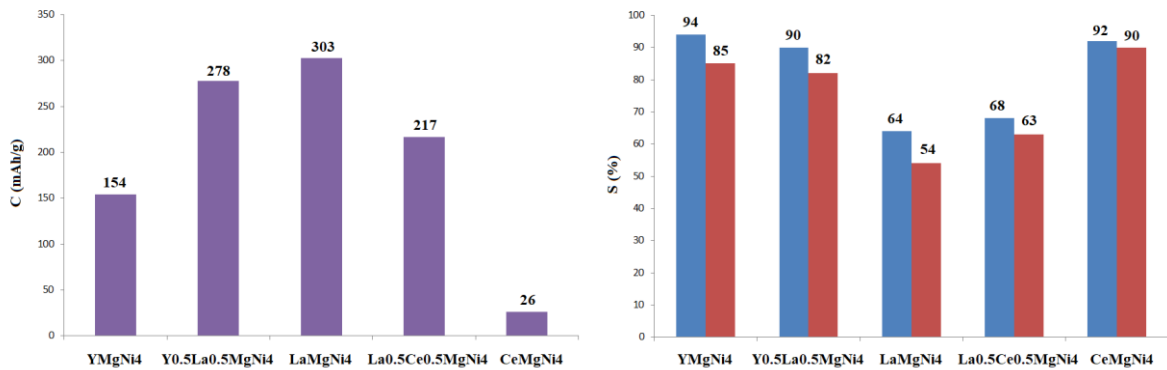**Fig. 5.** High rate dischargeability of the $R_{1-x}R'_xMgNi_{4-y}Co_y$ alloys.



**Fig. 6.** Maximum discharge capacity (*a*) and cyclic stability after $30^{th}$ (first columns) and $50^{th}$ (second columns) cycles of the $R_{1-x}R'_xMgNi_4$ electrodes (*b*).

that the increase in Co content impairs the electrochemical kinetics and reduces the dehydriding process of the alloy electrode.

Finally, the obtained results were compared with characteristics of the related compounds. The comparison diagrams of Co-free alloys is displayed in Fig. 6. It is seen that La-based alloys were demonstrated the highest discharge capacities. Maximum discharge capacity of LaMgNi₄ is 2 and 12 times more than YMgNi₄ and CeMgNi₄, respectively. However, the LaMgNi₄ electrode has poor cyclic stability comparing with YMgNi₄ and CeMgNi₄ ones. Substituted alloys La₀.₅Y₀.₅MgNi₄ and La₀.₅Ce₀.₅MgNi₄ are clearly characterized by better

electrochemical performance. Let's turn our attention to the Co-doped alloys. Fig. 7 displays summarized electrochemical properties for the $R_{1-x}R'_xMgNi_3Co$ electrodes. The YMgNi₃Co and CeMgNi₃Co electrodes exhibit low values of discharge capacity. Maximum discharge capacity of other electrodes didn't exceed 300 mA·h/g; indicatively the highest one had the La₀.₅Y₀.₅MgNi₃Co electrodes. It can be note that during cycling processes the Y- and Pr-based alloys lost less capacity, while the La- and Nd-based ones demonstrated greater decay of discharge capacity. Interesting that CeMgNi₄ and CeMgNi₃Co electrodes with extremely small initial capacity showed the best cycling.
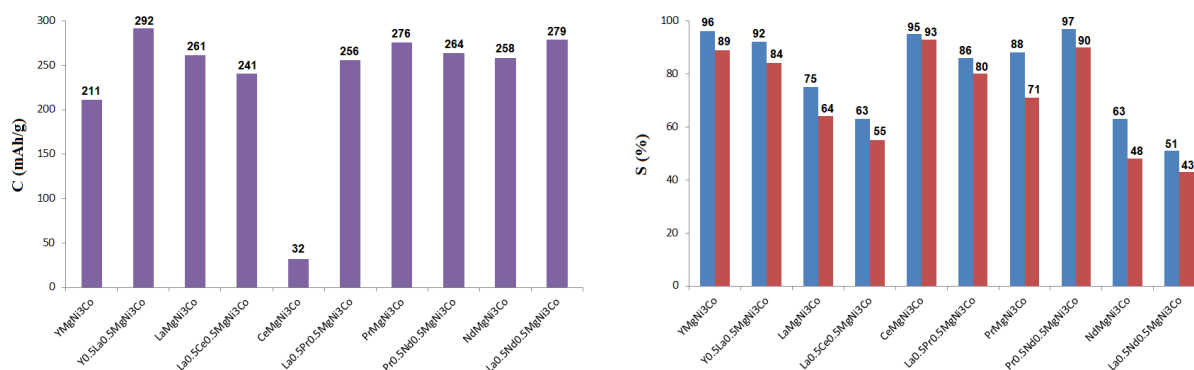
**Fig. 7.** Maximum discharge capacity (*a*) and cyclic stability after 30th (first columns) and 50th (second columns) cycles of the $R_{1-x}R'_xMgNi_3Co$ electrodes (*b*).

## Conclusion

The influence of Co substitution on the structural properties of $R_{1-x}R'_xMgNi_{4-y}Co_y$ (R, R' = Y, La, Ce; $x = 0.5$; $y = 0, 1, 2$) alloys and their hydrides has been investigated. The hydrogenation by solid–gas method of these alloys resulted in the formation of $La_{0.5}Y_{0.5}MgNi_4H_{4.31}$, $La_{0.5}Y_{0.5}MgNi_3CoH_{4.85}$, $La_{0.5}Y_{0.5}MgNi_2Co_2H_{5.18}$, $La_{0.5}Ce_{0.5}MgNi_3CoH_{6.40}$ and $La_{0.5}Ce_{0.5}MgNi_2Co_2H_{6.48}$ hydrides. Transformation from cubic to orthorhombic structure upon hydrogenation has been observed for the parent $La_{0.5}Y_{0.5}MgNi_4$ and $La_{0.5}Ce_{0.5}MgNi_4$ alloys, whereas it has been found that Co-containing hydrides preserved the parent cubic structure. It has been shown by electrochemical

investigation that substitution of the nickel atoms by the cobalt ones in $R_{1-x}R'_xMgNi_{4-y}Co_y$ slightly increase ($y = 1$) and then decrease ($y = 2$) discharge capacity. Higher capacity was seen for the $La_{0.5}Y_{0.5}MgNi_{4-y}Co_y$ electrodes; it varies between 277 and 292 mA·h/g. These electrodes demonstrated much better cyclic stability than that for the $La_{0.5}Y_{0.5}MgNi_{4-y}Co_y$ ones. The Co-free alloys is characterized by higher values of high rate dischargeability ($HRD_{1000} = 42 – 47$ %).

***Verbovytskyy Yu. -*** Senior Fellow, Ph.D;
***Zavaliy I.Yu. -*** Head of Department, Doctor of Chemistry;
***Berezovets V.V.*** – Research assistant, Ph.D;
***Lyutyy P.Ya.*** – Research assistant, Ph.D.

[1] T. Kohno, H. Yoshida, F. Kawashima, T. Inaba, I. Sakai, M. Yamamoto, M. Kanda, J. Alloys Compd. 311, 5 (2000) (https://doi.org/10.1016/S0925-8388(00)01119-1).

[2] B. Liao, Y.Q. Lei, L.X. Chen, G.L. Lu, H.G. Pan, Q.D. Wang, Electrochimica Acta 50, 1057 (2004) (https://doi.org/10.1016/j.electacta.2004.08.004).

[3] Y. Liu, Y. Cao, L. Huang, M. Gao, H. Pan, J. Alloys Compd. 509(3), 675 (2011) (https://doi.org/10.1016/j.jallcom.2010.08.157).

[4] Yu.V. Verbovytskyy, I.Yu. Zavaliy, Materials science 51(4), 443 (2016) (https://doi.org/10.1007/s11003-016-9861-0).

[5] Yu.V. Verbovytskyy, I.Yu. Zavaliy, Materials science 52(6), 747 (2017) (https://doi.org/10.1007/s11003-017-0018-6).

[6] L. Guéneé, V. Favre-Nicolin, K. Yvon, J. Alloys Compd. 348, 129 (2003) (https://doi.org/10.1016/S0925-8388(02)00797-1).

[7] Z.M. Wang, H.Y. Zhou, Z.F. Gu, G. Cheng, A.B. Yu, J. Alloys Compd. 377, L7 (2004) (https://doi.org/10.1016/j.jallcom.2004.01.048).

[8] Z.M. Wang, H.Y. Zhou, G. Cheng, Z.F. Gu, A.B. Yu, J. Alloys Compd. 384, 279 (2004) (https://doi.org/10.1016/j.jallcom.2004.04.087).

[9] S. Zhang, H. Zhou, Z. Wang, R.P. Zou, H. Xu, J. Alloys Compd. 398, 269 (2005) (https://doi.org/10.1016/j.jallcom.2005.02.015).

[10] Z.M. Wang, H. Zhou, R.P. Zou, Q. Yao, J. Alloys Compd. 429, 260 (2007) (https://doi.org/10.1016/j.jallcom.2006.03.094).

[11] J. Chotard, D. Sheptyakov, K. Yvon, Z. Kristallogr. 223, 690 (2008) (https://doi.org/10.1524/zkri.2008.1124).

[12] N. Terashita, K. Sakaki, S. Tsunokake, Y. Nakamura, E. Akiba, Mat. Trans. 53, 513 (2012) (https://doi.org/10.2320/matertrans.M2011334).

[13] K. Sakaki, N. Terashita, S. Tsunokake, Y. Nakamura, E. Akiba, J. Phys. Chem. C. 116, 19156 (2012) (https://doi.org/10.1021/jp3052856).

[14] K. Sakaki, N. Terashita, S. Tsunokake, Y. Nakamura, E. Akiba, J. Phys. Chem. C. 116, 1401 (2012) (https://doi.org/10.1021/jp206446c).

[15] J. Tan, X. Zeng, J. Zou, X. Wu, W. Ding, Trans. Nonferrous Met. Soc. China. 23, 2307 (2013) (https://doi.org/10.1016/S1003-6326(13)62733-8).

[16] T. Yang, T. Zhai, Z. Yuan, W. Bu, S. Xu, Y. Zhang, J. Alloys Compd. 617, 29 (2014) (https://doi.org/10.1016/j.jallcom.2014.07.206).

[17] T. Zhai, T. Yang, Z. Yuan, Y. Zhang, Int. J. Hy-drogen Energy 39, 14282 (2014) (https://doi.org/10.1016/j.ijhydene.2014.03.039).

[18] Q. Zhang, Z. Chen, Y. Li, F. Fang, D. Sun, L. Ouyang, M. Zhu, J. Phys. Chem. C. 119, 4719 (2015) (https://doi.org/10.1021/acs.jpcc.5b00279).

[19] V.V. Shtender, R.V. Denys, V. Paul-Boncour, A.B. Riabov, I.Yu. Zavaliy, J. Alloys Compd. 603, 7 (2014) (https://doi.org/10.1016/j.jallcom.2014.03.030).

[20] Yu.V. Verbovytskyy, V.V. Shtender, P.Ya. Lyutyy, I.Yu. Zavaliy, Powder Met. Met. Ceramics 55(10-11), 559 (2017) (https://doi.org/10.1007/s11106-017-9839-y).

[21] V.V. Shtender, R.V. Denys, V. Paul-Boncour, Yu.V. Verbovytskyy, I.Yu. Zavaliy, J. Alloys Compd. 639, 526 (2015) (https://doi.org/10.1016/j.jallcom.2015.03.187).

[22] Yu.V. Verbovytskyy, V.V. Shtender, A. Hackemer, H. Drulis, I.Yu. Zavaliy, P.Ya. Lyutyy, J. Alloys Compd. 741, 307 (2018) 307−314 (https://doi.org/10.1016/j.jallcom.2018.01.067).

[23] V.O. Oprysk, Yu.V. Verbovytskyy, V.V. Shtender, P.Ya. Lyutyy, I.Yu. Zavaliy, Solid State Sci. 84, 112 (2018) (https://doi.org/10.1016/j.solidstatesciences.2018.08.009).

[24] J. Rodriguez-Carvajal, T. Roisnel (International Union for Crystallography, 1998).

[25] P. Villars, K. Cenzual (ASM International, Materials Park, OH, 2014).

Ю.В. Вербовицький, І.Ю. Завалій, В.В. Березовець, П.Я. Лютий

# Газове та електрохімічне гідрування сплавів $R_{1-x}R'_xMgNi_{4-y}Co_y$ (R, R' = Y, La, Ce)

*Фізико-механічний інститут ім. Г.В. Карпенка НАН України, Львів, Україна, yuryvv@bigmir.net*

Нові сплави $R_{1-x}R'_xMgNi_{4-y}Co_y$ (R, R' = Y, La, Ce; $x = 0.5$; $y = 0, 1, 2$) синтезували методом порошкового спікання, для яких досліджено кристалічну структуру та воденьсорбційні властивості. Рентгенівським дифракційним методом порошку визначено кристалічну структуру фаз $R_{1-x}R'_xMgNi_{4-y}Co_y$ (структурний тип $MgCu_4Sn$). Синтезовані сплави поглинають водень при кімнатній температурі та тиску водню 0,1 - 10 бар. Для деяких досліджуваних сполук виявлено утворення гідридів з кубічною та орторомбічною структурами. Найбільший вміст водню виявлено для сполук, в яких половина нікелю заміщена на кобальт: $La_{0.5}Y_{0.5}MgNi_2Co_2H_{5.18}$ та $La_{0.5}Ce_{0.5}MgNi_2Co_2H_{6.48}$. Електрохімічні дослідження показали, що електродні матеріали з ітрієм мають кращу електрохімічну ємність порівняно зі сплавами, які леговані церієм. Найвищу розрядну ємність 292 мАгод/г спостерігали для $La_{0.5}Y_{0.5}MgNi_3Co$, однак найкращу циклічну стабільність після 50-го циклу (92 %) виявили для $La_{0.5}Y_{0.5}MgNi_2Co_2$. Отримані електрохімічні параметри порівнювали з такими для споріднених сполук. Високошвидкісна розрядна здатність сплавів, що містили лише нікель, була вдвічі більшою при I = 1 А/г від такої для легованих кобальтом матеріалів.

**Ключові слова:** рідкісноземельні сполуки, сполуки магнію, кристалічна структура, гідрування сплавів, металогідридні електроди.